

Neural Autoregressive Flows for Markov Boundary Learning

Khoa Nguyen¹, Bao Duong¹, Viet Huynh², Thin Nguyen¹

¹Deakin Applied Artificial Intelligence Initiative, Geelong, Australia

²Edith Cowan University, Perth, Australia

{khoa.nguyen, b.duong, thin.nguyen}@deakin.edu.au, v.huynh@ecu.edu.au

Abstract—Recovering Markov boundary—the minimal set of variables that maximizes predictive performance for a response variable—is crucial in many applications. While recent advances improve upon traditional constraint-based techniques by scoring local causal structures, they still rely on nonparametric estimators and heuristic searches, lacking theoretical guarantees for reliability. This paper investigates a framework for efficient Markov boundary discovery by integrating conditional entropy from information theory as a scoring criterion. We design a novel masked autoregressive network to capture complex dependencies. A parallelizable greedy search strategy in polynomial time is proposed, supported by analytical evidence. We also discuss how initializing a graph with learned Markov boundaries accelerates the convergence of causal discovery. Comprehensive evaluations on real-world and synthetic datasets demonstrate the scalability and superior performance of our method in both Markov boundary discovery and causal discovery tasks.

Index Terms—Markov boundary, Markov blanket, causal discovery, information theoretic learning, autoregressive modeling, causal feature selection.

I. INTRODUCTION

The Markov Blanket, introduced by Pearl [31] in causal Bayesian networks, is a set S that captures the local causal mechanisms for a variable T and statistically shields T from the rest of the system $V \setminus S$: $T \perp\!\!\!\perp V \setminus S \mid S$ [18], [31]. The Markov boundary (MB) is defined as the minimal Markov blanket.¹ MBs are crucial in a wide range of domains, including bioinformatics [21], neuroscience [16], and environmental science [33]. In the realm of data science and causality, they are prevalently applied in causal feature selection [44], increasingly in missing data imputation [22], divide-and-conquer causal discovery [11], and LLM reasoning [20]. Under standard faithfulness assumptions, the MB of a variable is unique without the need for additional experimental data [39]; thus, it is theoretically feasible to design a learning algorithm \mathcal{L}^* that approximates the optimal solution with sufficient observational data. However, MB learning faces significant challenges in large graphs with nonlinear dependencies and unknown associated data distributions, which complicate accurate and scalable inference [43].

Traditionally, MB learning in the constraint-based approach indirectly uses pairwise conditional independence (CI) tests. This direction [23], [32], [38], [39], [42] has a solid theoretical

foundation but relies on the accuracy of these tests, making it susceptible to restricted assumptions about data distribution, insufficient training samples, and the scale of the separating set [43]. The sequential decision-making process can lead to cascading errors and ignoring true positives [43].

Score-based approaches, which evolved later but received limited attention, identify local causal structures by optimizing a quantifiable objective [14], [43]. However, commonly used scoring criteria, such as BDeu and BDe, impose strict assumptions on the data, mainly designed for discrete or linear Gaussian data [43]. Recently, KMB [43] was proposed to address the complexity of data relationships. It, however, employs the conditional covariance operator (CCO), a kernel-based design known for its inefficiency in terms of sample size and dimensionality [12]. The learning mechanism of KMB relies on a heuristic algorithm lacking theoretical justification and must solve a continuous relaxation-based objective at each step of evolving its predicted MB. This leads to inefficiencies in learning MBs for all variables in the network.

Regarding the applicability of MBs in follow-up tasks, we focus on their integration as a warm-start step in causal discovery (CD) [1], [32], [39]. The key advantage lies in guiding CD within a reduced search space by eliminating obviously irrelevant relationships [1], [39]. From an overarching technical viewpoint, this group has evolved alongside constraint-based MB learning, which approaches CD by first solving the local causal induction problem and then adopting a local-to-global learning strategy. As a subset of constraint-based CD, a critical component of these techniques is the pairwise CI test, where greater efficiency reflects a reduction in the number of required trials [1], [25]. In the emerging field of differentiable causal discovery (DCD), state-of-the-art techniques employ MB learning to construct the moral graph, which serves as a mask for subsequent DAG estimation [2], [26]. SDCD [26] has demonstrated improved stability and scalability, particularly for sparse graphs common in real-world scenarios. However, the moral graphs learned during preselection are not true MB-derived moral graphs but rather sparser approximations that eliminate some false positives while avoiding a complete graph, due to the inherent limitations of DCD [41].

We address the gaps across these worlds: our method advances a novel class of autoregressive flow-based generative models, aligning them with conditional entropy from classic information theory to derive a theoretically justified scoring

¹Some literature refers to this minimal set as the Markov blanket [18], [44]. To distinguish it from larger sets, we adopt the Markov boundary definition from [31], and use the abbreviation MB for Markov boundary.

objective. We introduce *Any-subset Masked Autoregressive Flows*, also known as **Flows for ANy-Subset (FANS)**, which efficiently model nonlinear relationships and noise distributions through latent representation learning, thereby transforming intractable universal entropy into an easily estimable counterpart. A single trained **FANS** can also estimate any conditional entropy $H(T|\mathbf{S})$, where T is an arbitrary random variable and \mathbf{S} is any subset of variables. This enables its use in our greedy algorithm, **FANS-based Information gaThEring for MB discovery (FANSITEMB)**, facilitating seamless integration into CD pipelines, unlike previous score-based approaches that require separate models for each variable [43].

Our main contributions are:

- **FANS**,² a neural model redesigned from original autoregressive flows [17]. It combines strengths from both masked autoregressive autoencoder neural networks [15] and normalizing flows [29], enhancing expressiveness and efficacy in approximating underlying distributions. With amortized training, **FANS** can *estimate conditional entropy of arbitrary variables conditioned on any subsets, thereby avoiding the computational expense of learning a separate model for each subset*. Its compact design also reduces parameters, optimizing computational efficiency when dealing with sparse Bayesian networks.
- **FANSITEMB**, a greedy and parallelizable algorithm for discovering MBs in polynomial time, supported by a thorough theoretical analysis of error bounds.
- **FANSITE-DCD**, a MB-based differentiable causal discovery method adapted from SDCD, ensuring learning of DAGs from a minimal I-map-based subspace.
- Empirical evidence on the effectiveness of the proposed framework across various synthetic settings and four real-world gene regulatory networks.

II. RELATED WORKS

A significant portion of MB discovery focuses on constraint-based algorithms that identify MBs by mining conditional independence (CI) relations. As a crucial component of such group, the correctness of every CI test must be assumed, with χ^2 -tests and G^2 -tests commonly employed for discrete cases, and Fisher’s Z-test used for continuous cases under the assumption of linear relationships and additive Gaussian noise. Growing-Shrink (GS) [23] was the first sound MB learning algorithm, subsequently improved by the IAMB family [38]. A straightforward approach, Total Conditioning (TC) [32], states that $X \in \mathcal{MB}_Y$ and $Y \in \mathcal{MB}_X \iff X \not\perp\!\!\!\perp Y \mid \mathbf{V} \setminus \{X, Y\}$. Despite possessing a theoretical foundation thanks to fine-grained pairwise testing, these methods require a sample size that is exponential to the MB size and necessitate $\mathcal{O}(d^2)$ CI tests, where each test may involve conditioning on a large variable set. EEMB [42] recently proposed simultaneous learning of the parent-child and spouse sets, achieving superior accuracy compared to other methods in this group.

Score-based MB learners are central to curiosity-driven research as they design specific scoring functions to directly identify the MB of a target, though the literature remains sparse. The key motivation stems from the uniqueness of MB under the faithfulness assumption, making it theoretically feasible to solve a formal objective for obtaining an optimal solution: the smallest subset representing the MB. This problem, however, is fundamentally a combinatorial optimization task, which is NP-hard and computationally intractable in polynomial time. Regarding scoring criteria, SLL [27] and S²TMB [14] utilized BDeu, a decomposable score commonly used in Bayesian structure learning and specifically tailored for discrete data. Another widely adopted score, the Minimum Message Length (MML), was integrated in [19] and demonstrated to be locally consistent under specific conditions. Recently, the authors of KMB [43] established that the MB corresponds to the feature subset minimizing the conditional covariance operator (CCO) $\Sigma_{TT|\mathbf{S}}$ when embedding variables from a Euclidean space into a reproducing kernel Hilbert space (RKHS). Formally, both the target space \mathcal{T} and feature space \mathcal{S} are mapped into RKHS spaces $\mathcal{H}_{\mathcal{T}}$ and $\mathcal{H}_{\mathcal{S}}$ using positive definite kernels. For $\forall g \in \mathcal{H}_{\mathcal{T}}$, $\langle g, \Sigma_{TT|\mathcal{MB}g} \rangle_{\mathcal{H}_{\mathcal{T}}} = \langle g, \Sigma_{TT|\mathbf{V}g} \rangle_{\mathcal{H}_{\mathcal{T}}}$. Although kernel-based characterization can capture nonlinear relationships, their performance is constrained by kernel selection and suffers from scalability issues. Except for S²TMB [14], none of these methods guarantee the correctness of their follow-up algorithms in approximating the MB along with their provided scores. The heuristic-based search algorithm in KMB [43] must solve its objective with every operation on the evolving MB (i.e., removing or adding a node), which is computationally inefficient.

MB-based causal discovery (CD) can be categorized into three approaches. For constraint-based methods, the state-of-the-art MARVEL [25] leverages MB information for recursive learning through removable variables, reducing the number of CI tests to $\mathcal{O}(d\Delta_{in}^2 2^{\Delta_{in}^2})$, whereas other constraint-based algorithms require at least $\mathcal{O}(d^2\Delta_{in}^2 2^{\Delta_{in}^2})$ (where d and Δ_{in} are the number of variables and the maximum in-degree of the causal DAG). An emerging group, including SDCD [26] and DAT [2], employs MB-derived moral graphs to mask their differentiable CD models. They transform MB learning into a sparse regression problem to enable expressive neural network integration. As noted, this process is essentially a graph pruning step based on the SEM assumption. Finally, another line of methods, DCILP [11], utilizes MBs to partition the graph into subgraphs, enabling parallelized CD.

Our work advances these fields by proposing a new family of masked autoregressive flows—a subclass of normalizing flows that has gained attention for its efficacy in density estimation and variational inference [9], [17]. Our models can estimate arbitrary conditional entropy and work in conjunction with an efficient greedy search algorithm. Normalizing flows have intersected with information theory in various studies, particularly in mutual information estimation [12], demonstrating superior accuracy, especially with continuous random

²<https://github.com/khoangdadk/FANS>

variables. We, in turn, also focus on the continuous instance of the problem, as noted in [12], which is more challenging due to the unknown closed-form of data density. Furthermore, we demonstrate how our robust MB learners enhance DAG searching from the perspective of CD.

III. METHODOLOGY

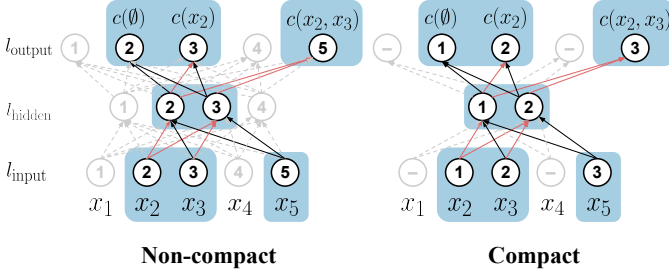


Fig. 1. Illustration of weight masking mechanism in FANS, as described in Subsection III-B2, for specific subset $\mathbf{S} = \{X_2, X_3, X_5\}$. This simplifies the original illustration of MADE architecture for better visualization, showing only a hidden layer with a block of nodes and output layer with a block of nodes. Full autoencoder may consist of multiple hidden layers, each with several blocks of hidden nodes, which can be permuted, as shown in Fig. 1 from [15]. Solid connections represent fully-connected weight regions in Step 1, while red connections indicate autoregressive masks in Step 2. Other subsets will have different masks. In compact version (right figure), assuming maximum size of observed subsets is 3, each block of hidden layer reduces to 2 nodes. Original element indices of \mathbf{S} are rescaled and colliders resolved: $[2, 3, 5] \rightarrow \left[\left[\frac{2*2}{5-1} \right], \left[\frac{3*2}{5-1} \right], \left[\frac{5*2}{5-1} \right] \right] \rightarrow [1, 2, 3]$.

Regarding notation, we use capitalized letters X, Y , etc., for random variables; their bold counterparts \mathbf{X}, \mathbf{Y} , etc., for sets of variables; lowercase letters x, y , etc., for the realizations of those variables; and bold lowercase letters \mathbf{x}, \mathbf{y} , etc., for realization vectors of sets. Let us begin with the formal statement of Markov boundary discovery problem. As input, we have N d -dimensional observations $\mathcal{D} = \{\mathbf{x}^{(k)}\}_{k=1}^N$, sampled i.i.d. from an unknown joint distribution \mathbf{P} that is faithful to a corresponding causal Bayesian network (CBN) \mathcal{G} . The goal is to identify the MB for every variable X_i .

Definition 1 (Markov boundary (MB)). Given a DAG \mathcal{G} and a distribution \mathbf{P} that are faithful to each other, the MB of each target X , denoted as \mathcal{MB}_X , is *unique* and consists of its parents Pa_X , children Ch_X , and co-parents (spouses) Sp_X : $\mathcal{MB}_X = Pa_X \cup Ch_X \cup Sp_X$.

A. Conditional entropy as a scoring criterion

We begin by presenting the key observation that underlies the development of our method.

Theorem 2. *The MB $\mathcal{MB}_T \subset \mathbf{V}$ of random variable $T \in \mathbf{V}$ is the subset $\mathbf{S} \subset \mathbf{V} \setminus \{T\}$ that minimizes $H(T | \mathbf{S})$, where $H(\cdot | \cdot)$ is the conditional entropy. Furthermore, $\forall \mathbf{S}' \subseteq \mathbf{V} \setminus \{T\}$ that satisfy $\mathcal{MB}_T \subseteq \mathbf{S}'$, we have: $H(T | \mathbf{S}') = H(T | \mathcal{MB}_T)$.*

The proof is provided in the Appendix A-A.

It is worth emphasizing that estimating conditional entropy is equivalent to estimating the difference between two marginal entropies. In the special case of Gaussian random vectors, i.e.,

assuming that the functional form of the underlying CBN data-generating process is given by a linear Gaussian additive noise model $y = f(x) + \epsilon$, where $f(x) = \mathbf{w}^T \mathbf{x} + b$ and $\epsilon \sim \mathcal{N}(\mu, \sigma^2)$, it is straightforward to derive $H(T | \mathbf{S})$ using the entropy of a multivariate Gaussian distribution. Given $\mathbf{x} \sim \mathcal{N}(\boldsymbol{\mu}, \boldsymbol{\Sigma})$, $H(\mathbf{x}) = \frac{d}{2} (1 + \log(2\pi)) + \frac{1}{2} \log \det \boldsymbol{\Sigma}$. Let $\boldsymbol{\Sigma}_{\mathbf{S}}$ represent the sub-matrix of the covariance matrix $\boldsymbol{\Sigma}$ with row and column set \mathbf{S} . From $H(T | \mathbf{S}) = H(T, \mathbf{S}) - H(\mathbf{S})$, we can derive:

$$H(T | \mathbf{S}) = \frac{1}{2} \left(1 + \log(2\pi) + \log \frac{\det \boldsymbol{\Sigma}_{\{T\} \cup \mathbf{S}}}{\det \boldsymbol{\Sigma}_{\mathbf{S}}} \right) \quad (1)$$

Practically, the problem is not simple as real-world CBNs may not adhere to a deterministic data-generating process, rendering their closed forms intractable. In these situations, relationships between continuous random variables are often complex and nonlinear, with unknown endogenous noise distributions. **RQ1.** How can we estimate the conditional entropy in such cases? Our key idea is to leverage the expressiveness and tractability of latent representation learning through *masked autoregressive flows*.

B. Conditional entropy neural estimator design

In this subsection, we explain how a masked autoregressive flow (MAF) map continuous random variables from multimodal distributions into standard Gaussian space, facilitating conditional entropy estimation for any underlying distribution. We then introduce our novel class of MAFs tailored for MB discovery: the **FANS** model.

1) *Universal conditional entropy estimation:* At the core of our design are MAFs [9], [17], [30], which have gained significant attention in recent years for critical applications such as density estimation and variational inference. MAFs harmonize the strengths of normalizing flows [29] and autoregressive models [15], offering advantages from both approaches: the former allows compositions of many invertible transformations with a tractable Jacobian, and the latter facilitates the integration of expressive neural architectures while maintaining efficient GPU training. Consequently, MAFs function as *tractable universal density approximators* with arbitrary non-zero precision [9], [17], [30]. In principle, autoregressive modeling first decomposes a joint density $p(\mathbf{x})$ into a product of univariate conditionals: $p(\mathbf{x}) = \prod_i p(x_i | \mathbf{x}_{<i})$, where each univariate conditional $p(x_i | \mathbf{x}_{<i})$ is transformed into a base density (e.g., a standard Gaussian) via a conditional diffeomorphic transformation,³ parametrized by $\mathbf{x}_{<i}$, $f_{\mathbf{x}_{<i}} : x_i \mapsto u_i$:

$$p(x_i | \mathbf{x}_{<i}) = p_{u_i}(u_i) \left| \det \frac{\partial f_{\mathbf{x}_{<i}}}{\partial x_i} \right| \quad (2)$$

where $u_i = f_{\mathbf{x}_{<i}}(x_i) = \tau(x_i, c(\mathbf{x}_{<i}))$. Two key features stand out: (1) Such transformation can be deepened by composing multiple single ones: $f = f_k \circ \dots \circ f_2 \circ f_1$, and (2) The autoregressive decomposition ensures that each dimension u_i of the transformed joint density also follows the base distribution. The autoregressive conditioner c is implemented

³A diffeomorphic transformation is a map $\tau(\cdot) : X \rightarrow X'$ that is differentiable, invertible, and has a differentiable inverse.

as a masked autoencoder (MADE) [15], which takes a vector \mathbf{x} as input and efficiently computes $c(\mathbf{x}_{<i})$ for all conditionals within a forward pass. The transformer τ can be an affine transformation: $u_i = \mu + \sigma x_i$ [30], where μ and σ are outputs of $c(\mathbf{x}_{<i})$; or a more expressive transformation: $u_i = \sigma^{-1}(w^\top \cdot \sigma(a \cdot x_i + b))$ [17], where σ is a Lipschitz continuous activation function (e.g., sigmoid), and w, a, b are output vectors from $c(\mathbf{x}_{<i})$, with w and a being positive vectors. Notably, the autoregressive structure ensures that the Jacobian of transformation \mathcal{F} on multivariate inputs is triangular by design, making its determinant easily computable:

$$\left| \det \frac{\partial \mathcal{F}}{\partial \mathbf{x}} \right| = \left| \prod_i \frac{\partial f_{\mathbf{x}_{<i}}}{\partial x_i} \right| \quad (3)$$

We will briefly denote $\partial f_{\mathbf{x}_{<i}}/\partial x_i$ as $\partial f/\partial x_i$ for simplicity.

Rendering universal conditional entropy tractable. Given the target variable $T \in \mathbf{V}$, consider a diffeomorphism $\mathcal{F}_{\mathbf{S}} : \mathbf{x}_{\mathbf{S}} \mapsto \mathbf{u}_{\mathbf{S}}$, where $\mathbf{S} \subseteq \mathbf{V} \setminus \{T\}$. We initially observe:

$$H(\mathbf{S}) = H_{\mathbf{u}}(\mathbf{S}) - \mathbb{E}_{p(\mathbf{x}_{\mathbf{S}})} \log \left| \det \frac{\partial \mathcal{F}_{\mathbf{S}}}{\partial \mathbf{x}_{\mathbf{S}}} \right| \quad (4)$$

where $\mathbf{x}_{\mathbf{S}}$ represents the vector part w.r.t \mathbf{S} . Assuming every $\mathcal{F}_{\mathbf{S}}$ maps $\mathbf{x}_{\mathbf{S}}$ to $\mathbf{u}_{\mathbf{S}}$ in an isometric Gaussian space such that $\mathbf{u}_{\mathbf{S}} \sim \mathcal{N}(0, \mathbf{I}_{\mathbf{u}_{\mathbf{S}}})$, we can assert that $H_{\mathbf{u}}(\mathbf{S}) = \frac{1}{2}(1 + \log(2\pi))$. Let $\mathbf{TS} := \{T\} \cup \mathbf{S}$; the conditional entropy $H(T|\mathbf{S})$ for the general case is derived from Eq. 4 as follows:

$$\begin{aligned} H(T|\mathbf{S}) &= \mathbb{E}_{p(\mathbf{x}_{\mathbf{S}})} \log \left| \det \frac{\partial \mathcal{F}_{\mathbf{S}}}{\partial \mathbf{x}_{\mathbf{S}}} \right| - \mathbb{E}_{p(\mathbf{x}_{\mathbf{TS}})} \log \left| \det \frac{\partial \mathcal{F}_{\mathbf{TS}}}{\partial \mathbf{x}_{\mathbf{TS}}} \right| \\ &= \mathbb{E}_{p(\mathbf{x}_{\mathbf{TS}})} \left[\log \left| \det \frac{\partial \mathcal{F}_{\mathbf{S}}}{\partial \mathbf{x}_{\mathbf{S}}} \right| - \log \left| \det \frac{\partial \mathcal{F}_{\mathbf{TS}}}{\partial \mathbf{x}_{\mathbf{TS}}} \right| \right] \\ &= \mathbb{E}_{p(\mathbf{x}_{\mathbf{TS}})} \left[\sum_{X_i \in \mathbf{S}} \log \left| \frac{\partial f_{\mathbf{S}}}{\partial x_i} \right| - \sum_{X_j \in \mathbf{TS}} \log \left| \frac{\partial f_{\mathbf{TS}}}{\partial x_j} \right| \right] \end{aligned} \quad (5)$$

noting that $f_{\mathbf{S}}(x_i) = \tau(x_i, c(\mathbf{x}_{<i}))$ with $X_i \in \mathbf{S}$ and $\mathbf{X}_{<i} \subset \mathbf{S}$ including only of the variables prior to X_i when decomposing $p(\mathbf{x}_{\mathbf{S}})$ into conditionals. Inference from line 2 to line 3 of Eq. 5 is based on the results of Eq. 3. Tractable functions $\mathcal{F}_{\mathbf{S}}$ and $\mathcal{F}_{\mathbf{TS}}$ from trained MAFs, which are inherently designed for easy partial derivative computation, enable efficient estimation of $H(T|\mathbf{S})$ via Eq. 5 using Monte Carlo integration on K i.i.d. observations uniformly sampled from \mathcal{D} , where $\mathbf{x}^{(k)} = [x_1^{(k)}, x_2^{(k)}, \dots, x_d^{(k)}] \forall k \in [K]$. Accordingly,

$$H(T|\mathbf{S}) \approx \frac{1}{K} \sum_{k=1}^K \left(\sum_{X_i \in \mathbf{S}} \log \left| \frac{\partial f_{\mathbf{S}}}{\partial x_i^{(k)}} \right| - \sum_{X_i \in \mathbf{TS}} \log \left| \frac{\partial f_{\mathbf{TS}}}{\partial x_i^{(k)}} \right| \right) \quad (6)$$

To obtain $|\partial f_{\mathbf{S}}/\partial x_i|$ in Eq. 5, it can be deduced from the MAF architecture that access to the univariate conditionals $p(x_i | \mathbf{x}_{<i})$ is necessary during the autoregressive decomposition via the chain rule, with $\mathbf{x}_{<i}$ being the realizations of $\mathbf{X}_{<i} \subset \mathbf{S}$ ordered prior to X_i within a specific variable order: this term essentially represents the residual generated by the change-of-variable in Eq. 2. It has been argued that

training an order-agnostic conditioner c is theoretically feasible and can provide access to all conditionals from any order [15], given that each order does not shuffle between stacks in normalizing flows. This scenario, however, is empirically inefficient, as stated by the authors in [36]; thus, it is evidently not employed by typical MAFs [9], [17], [30] in density estimation, particularly in high-dimensional spaces. For this reason, we focus on the default setting of these MAFs in [9], [17], [30], which preserves the original variable order of input $\pi(d) = [1, 2, \dots, d]$ during training. As a trade-off, this design inherently restricts the model to a single order and can only derive conditionals $p(x_i | \mathbf{x}_{<i})$ from $\pi(d)$.

Given a fixed order $\pi(d)$, an alternative solution is to obtain conditionals not from the joint but separately from marginals corresponding to subsets of \mathbf{V} [36]. An arbitrary subset \mathbf{S} can be rearranged to form a discontinuous sub-sequence of $\pi(d)$, denoted as $\pi_{\mathbf{S}}$, from which the marginal for \mathbf{S} can be decomposed to derive $|\partial f_{\mathbf{S}}/\partial x_i|$. A single MAF can be adapted to align with this intuition through a minor architectural modification: Given \mathbf{S} , we mask all $X_i \notin \mathbf{S}$ in input \mathbf{x} to zeros, then feed this into MADE conditioner to produce a chain of $c(\mathbf{x}_{<i})$. We assume that zero-masked positions in $\pi(d)$ contribute nothing to $c(\mathbf{x}_{<i})$, so this term embeds only information of $\mathbf{X}_{<i} \subset \mathbf{S}$ that precedes X_i in $\pi_{\mathbf{S}}$. Nonetheless, MADE [15] initially uses only a portion of the weights of its neural network (NN) for the joint input. Depending on this fixed pre-masking, this straightforward approach fails to fully utilize complete NN for all marginals, as empirically demonstrated in Fig. 2 for typical MAFs [9], [17].

2) *Efficient redesign of Any-Subset Masked Autoencoders:* Building on Subsection III-B1, we aim to enable the conditioner c to efficiently compute $c(\mathbf{x}_{<i})$ for any $X_i \in \mathbf{S}$, where $\mathbf{S} \subseteq \mathbf{V} \setminus \{T\}$, and $\mathbf{x}_{<i}$ represents the realizations of $\mathbf{X}_{<i}$ preceding X_i under order $\pi(d)$. For a sample $\mathbf{x}^{(k)}$ and subset \mathbf{S} , let $x_{\mathbf{S}}^{(k)} = [x_{i_1}^{(k)}, \dots, x_{i_{|\mathbf{S}|}}^{(k)}]$ denote the non-zero elements in the masked vector (with zero values for $X_i \notin \mathbf{S}$). We achieve this goal using a modified version of MADE capable of processing any $x_{\mathbf{S}}^{(k)}$, efficiently allocating neural autoencoder weights, propagating $x_{\mathbf{S}}^{(k)}$ through this weight region, and outputting $|\mathbf{S}|$ autoregressive terms: $c(\emptyset), c(x_{i_1}^{(k)}), \dots, c(x_{i_1}^{(k)}, \dots, x_{i_{|\mathbf{S}|}}^{(k)})$. **RQ2.** How can this modification be implemented?

FANS employs a robust dynamic weight masking mechanism, wherein the weight regions of the autoencoder are adaptively assigned to each subset \mathbf{S} . We draw on concepts from the Lottery Ticket Hypothesis [4], [13] and various pruning strategies, which identify a subset of valuable model connections: A masked neural network with more connections demonstrates greater expressiveness, enabling improved and faster learning from data. Intuitively, we establish two objectives for our weight assignment/masking strategy: (1) to greedily maximize the number of connections utilized across the entire neural autoencoder for all subsets \mathbf{S} , and (2) to ensure that the overlap between two subsets results in a greater shared connection in their respective masks/weight regions.

As illustrated in Fig. 1, **FANS** masking mechanism operates through two steps: **Step 1. Locate the fully-connected weight region:** For subset \mathbf{S} , we redefine $\pi_{\mathbf{S}} = [i_1, i_2, \dots, i_{|\mathbf{S}|}]$, where each $i_j \in [1, d]$, as its increasing list of variable positions—a discontinuous subsequence of $\pi(d)$. Each hidden node in layer l is assigned a score $s \in [1, d-1]$, with selected nodes having scores $s \in \pi_{\mathbf{S}} \setminus \{i_{|\mathbf{S}|}\}$. Similarly, nodes in the input and output layers have scores $s \in [1, d]$, with selected nodes having scores $s \in \pi_{\mathbf{S}}$. We only select connections between these chosen nodes across layers. **Step 2. Force autoregressive masking:** The fully-connected weight region between two consecutive layers is masked autoregressively, similar to MADE, ensuring that a higher-layer node (considered from input to output) with score s_h receives information from lower-layer nodes with scores $s_l \leq s_h$. The exception is from the highest hidden layer to the output layer, where $s_l < s_h$.

Enabling compactness. For the MB discovery task, the MB size is often considerably smaller than the total number of variables, particularly in large sparse causal networks, leading to the intuition that investigating only subsets \mathbf{S} with maximum size $\max |\mathbf{S}| \ll d$ is sufficient. Let M denote a hyperparameter related to the maximum size of observed subsets. Each hidden layer of the **compact FANS** requires approximately $\alpha_B(M-1)$ nodes instead of $\alpha_B(d-1)$ nodes, where α_B is the number of blocks in each hidden layer (see Fig. 1 for details), due to the reduced size of $\pi_{\mathbf{S}}$. With $\pi_{\mathbf{S}} = [i_1, i_2, \dots, i_{|\mathbf{S}|}]$, each hidden node from *Step 1* would have a score s that satisfies $s \in [1, M-1] \cap \pi_{\mathbf{S}}^{\%}$, where $\pi_{\mathbf{S}}^{\%} = \left[\left\lceil \frac{(M-1)i_1}{d-1} \right\rceil, \dots, \left\lceil \frac{(M-1)i_{|\mathbf{S}|}}{d-1} \right\rceil \right]$ is the rescaled counterpart of $\pi_{\mathbf{S}}$ from d -scale to M -scale. Rescaling may result in overlapping elements in $\pi_{\mathbf{S}}^{\%}$, leading to $|\pi_{\mathbf{S}}^{\%}| < |\mathbf{S}| - 1$, while at least $|\mathbf{S}| - 1$ nodes are needed within each block of a hidden layer to carry autoregressive information $(x_{i_1}), (x_{i_1}, x_{i_2}), \dots, (x_{i_1}, \dots, x_{i_{|\mathbf{S}|-1}})$. These colliders can be addressed by greedily adjusting element values in $\pi_{\mathbf{S}}^{\%}$ to fill possible gaps between them. For example, given $M-1 = 6$ and $\pi_{\mathbf{S}}^{\%} = [1, 1, 2, 6, 6]$, the values in $\pi_{\mathbf{S}}^{\%}$ are adjusted from both sides as follows: $[1, 1, 2, 6, 6] \rightarrow [1, 2, 3, 6, 6] \rightarrow [1, 2, 3, 5, 6]$. The efficacy of the compact version is demonstrated in Fig. 2.

Training objective with FANS masking mechanism. In alignment with the training objective for density estimation in other MAF models, **FANS** is trained by maximizing the total log likelihood on training data, effectively fitting $p(\mathbf{x})$ through the diffeomorphic transformation in Eq. 2. The base distribution is chosen to be standard Gaussian. Notably, data samples are stochastically masked using a uniform d -dimensional binary mask distribution to fit marginals corresponding to subsets \mathbf{S} . Let \mathcal{M} denote the uniform mask distribution, $M_{\mathbf{S}} \sim \mathcal{M}$ represent the binary mask for \mathbf{S} , and $\mathbf{x}_{M_{\mathbf{S}}} := M_{\mathbf{S}} \odot \mathbf{x}$. We maximize the log likelihood of this term using training data in \mathcal{D} :

$$\mathbb{E}_{\mathbf{x} \sim p(\mathbf{x})} \left[\log p_{\mathbf{u}}(f_{\theta}(\mathbf{x}_{M_{\mathbf{S}}}) \odot M_{\mathbf{S}}) + \sum_{X_i \in \mathbf{S}} \log \left| \frac{\partial f_{\theta}(\mathbf{x}_{M_{\mathbf{S}}})}{\partial x_i} \right| \right] \quad (7)$$

Remark 3. Sampling a mask $M_{\mathbf{S}}$ for \mathbf{S} to fit marginal $p(\mathbf{x}_{\mathbf{S}})$ also implicitly fits marginals $p(x_{\mathbf{S}_{-1}}), p(x_{\mathbf{S}_{-2}}), \dots$ of its prefix subsets $\mathbf{S}_{-1}, \mathbf{S}_{-2}, \dots$, where $\pi_{\mathbf{S}} = [i_1, \dots, i_{|\mathbf{S}|}]$ and $\pi_{\mathbf{S}_{-k}} = [i_1, \dots, i_{|\mathbf{S}|-k}]$. This is due to $p(\mathbf{x}_{\mathbf{S}}) = p(\mathbf{x}_{\mathbf{S}_{-1}})p(x_{i_{|\mathbf{S}|}} | \mathbf{x}_{\mathbf{S}_{-1}}) = p(\mathbf{x}_{\mathbf{S}_{-2}})p(x_{i_{|\mathbf{S}|-1}} | \mathbf{x}_{\mathbf{S}_{-2}})p(x_{i_{|\mathbf{S}|}} | \mathbf{x}_{\mathbf{S}_{-1}}) = \dots$. Define a *leaf-subset* \mathbf{S}_{leaf} as a subset that is not a prefix of any other subset except itself (e.g., leaf node [3, 4] in Fig. 2(c) of [36]). Uniformly sampling *leaf-masks* $M_{\mathbf{S}_{\text{leaf}}}$ is sufficient, reducing the combinatorial space of masks by half (empirically shown in Fig. 2). Additionally, partially observing subsets \mathbf{S} of size $|\mathbf{S}| \leq M \ll d$ is sufficient for sparse graphs. Combining these insights, our masking strategy efficiently operates within a small fraction of the exponential masking space.

C. Polynomial-time greedy minimization

Optimizing objectives with set-based solutions is an NP-hard combinatorial problem [6], [8]. To address this in polynomial time, two common approaches are (1) continuous relaxation [43], which learns a differentiable subset mask, and (2) greedy search [5], [6], [8], [35], which iteratively refines the predictive set. We adopt the latter due to the complex implementation of continuous relaxation in our high-dimensional settings and the lack of explicit control from challenges in regularization parameter tuning [8], [35]. Accordingly, we adopt a greedy approach, which is simple yet efficient. We reformulate MB discovery problem as a **sequential information minimization** task [6], [8], a framework demonstrated to perform well within information-theoretic learning paradigms and is theoretically near-optimal under certain noise assumptions [6], [35]. Thus, it provides a solid foundation for our error-bound theorem (see our Theorem 4).

We introduce **FANSITEMB** (Algorithm 1), which guarantees convergence to a minimal set \mathbf{S}^* predicting the true \mathcal{MB}_{X_i} by minimizing $H(X_i | \mathbf{S})$ (see our Theorem 5). In the optimal case, the *growing phase* can yield the set $\tilde{\mathcal{MB}}_{X_i}^+$ satisfying $\mathcal{MB}_{X_i} \subseteq \tilde{\mathcal{MB}}_{X_i}^+$, where $H(X_i | \tilde{\mathcal{MB}}_{X_i}^+) = H(X_i | \mathcal{MB}_{X_i}) = \min_{\mathbf{S} \subseteq \mathbf{V} \setminus \{X_i\}} H(X_i | \mathbf{S})$ (Theorem 2). The *shrinking phase* then removes redundant variables from $\tilde{\mathcal{MB}}_{X_i}^+$ with minimal impact on $H(X_i | \tilde{\mathcal{MB}}_{X_i}^+)$. For discovering MBs of all variables in a causal network, **FANSITEMB** can operate in a *distributed parallel setup*, running independently for each target variable, followed by symmetry correction: $X_i \in \mathcal{MB}_{X_j} \Leftrightarrow X_j \in \mathcal{MB}_{X_i}$. Additionally, it can exploit *GPU parallelism* by batch-computing $H(X_i | \mathbf{S} \cup \{X_j\})$ for all candidate variables X_j during each step of the growing and shrinking phases. This ensures a computational complexity of $\mathcal{O}(bM)$ for inferring MBs of all variables simultaneously, where b is the batch count and M is the estimated maximum size of an MB, as defined. Compared to the closely related KMB [43], which employs an iterative MB discovery strategy and requires solving its training objective at least M times per target X_i , **FANSITEMB** is significantly more efficient.

Theorem 4 (Error bound of **FANSITEMB**). *Given that \mathcal{F}_{θ}^* is a universal approximator in the model class of **FANS**, it*

can approximate any conditional entropy $H(X_i | \mathbf{S})$ from Eq. 5 with arbitrary precision, where $X_i \in \mathbf{V}$ and $\mathbf{S} \subseteq \mathbf{V} \setminus \{X_i\}$, with \mathbf{V} being the set of all variables under a faithful distribution. Assuming the growing phase of Algorithm 1 stops at a subset $\tilde{\mathcal{M}}\mathcal{B}_{X_i}^+ \subset \mathbf{V} \setminus \{X_i\}$ where $|\tilde{\mathcal{M}}\mathcal{B}_{X_i}^+| = k'$, let $\mathcal{M}\mathcal{B}_{X_i}$ denote the true MB of X_i , referred to as the optimal solution of Algorithm 1, with $|\mathcal{M}\mathcal{B}_{X_i}| = k$. In the general case, for any $\delta > 0$, an estimation bound can be directly derived from Theorem 2 in [6]:

$$0 \leq H(X_i | \tilde{\mathcal{M}}\mathcal{B}_{X_i}^+) - H(X_i | \mathcal{M}\mathcal{B}_{X_i}) \leq \delta_e + \Delta_N$$

where $\Delta_N := \log N \left[1 - \exp\left(-\frac{k'}{k\gamma \max\{\log N, \log(1/\delta_e)\}}\right) \right]$, and γ is a constant that depends on the measurement noise from N samples. In the case of linear Gaussian additive noise, we can also derive a bound on the ratio between exponential terms as follows:

$$1 \leq \frac{2\pi e \sigma_{X_i}^2 - e^{2H(X_i | \mathcal{M}\mathcal{B}_{X_i})}}{2\pi e \sigma_{X_i}^2 - e^{2H(X_i | \tilde{\mathcal{M}}\mathcal{B}_{X_i}^+)}} \leq \frac{1}{1 - e^{-\lambda_{\min}(\mathbf{C}, 2k')}}}$$

where σ_{X_i} is the standard deviation of X_i and $\lambda_{\min}(\mathbf{C}, 2k')$ is the smallest eigenvalue among all $2k' \times 2k'$ sub-matrices of the joint covariance matrix after standardization, i.e., the correlation matrix \mathbf{C} .

We provide the proof in the Appendix A-B.

If $k' \geq k\gamma \max\left\{\log N, \log \frac{1}{\delta_e}\right\} \ln\left(\frac{\log N}{\delta_e}\right)$, then $H(X_i | \tilde{\mathcal{M}}\mathcal{B}_{X_i}^+) - H(X_i | \mathcal{M}\mathcal{B}_{X_i}) \leq 2\delta_e$ [6]. Hence, up to δ_e in absolute terms, we can approach the optimal MB achievable within $k = |\mathcal{M}\mathcal{B}_{X_i}|$ steps by expanding $\tilde{\mathcal{M}}\mathcal{B}_{X_i}^+$ sufficiently, within a logarithmic factor of k . In the linear Gaussian case, additional insights emerge: for sparse networks, where variables exhibit weaker correlations or independence, $\lambda_{\min}(\mathbf{C}, 2k')$ tends to be larger, yielding a tighter upper bound.

Theorem 5 (Soundness of FANSITEMB). *Under faithfulness, causal sufficiency, and \mathcal{F}_0^* as defined in Theorem 4, Algorithm 1 discovers all and only variables in the MB of the target node.*

The proof is provided in the Appendix A-C.

D. Differential causal discovery (DCD) with minimal I-map-based initialization

We investigate the integration of MB discovery with DCD, a recent advancement in causal discovery (CD). Principally, MB discovery serves as a preselection step, reducing the graph space to enhance numerical stability and scalability in DAG estimation. SDCD [26] and DAT [2] employ sparse regression objectives to learn MBs. DAT [2] minimizes: $\mathcal{L}_n(\theta_n) = \mathbb{E}[X^n - f_{\theta_n}(X^m)_{m \neq n}]^2 + \lambda \sum |W_{i,j}^n|$ while SDCD [26] optimizes $\mathcal{L}_n(\theta_n) = -\mathbb{E}[p_n(x_n | x_{-n}; \theta_n)] + \lambda \sum |W_{i,j}^n|$ where λ is the regularization term and $W_{i,j}$ denotes adjacency matrix weights. The warm-up step of SDCD and DAT has key limitations: (1) a single regularization term controls sparsity uniformly, ignoring MB size variation (e.g., smaller MBs may need larger λ , larger MBs require smaller λ); (2) SEM-derived

Algorithm 1 FANSITEMB for a single target

Input: Target $X_i \in \mathbf{V}$, K i.i.d. data samples in $\mathcal{D}_K \subseteq \mathcal{D}$, trained approximator f_θ , subset size threshold M , growing stop threshold ϵ_g , shrinking stop threshold ϵ_s , patience coefficient ρ .

Output: Predicted MB $\tilde{\mathcal{M}}\mathcal{B}_{X_i}$.

1: Initialize $\tilde{\mathcal{M}}\mathcal{B}_{X_i} \leftarrow \emptyset$, patience $\leftarrow 0$.

Growing phase

2: **while** exists $X_j \in \mathbf{V} \setminus (\{X_i\} \cup \tilde{\mathcal{M}}\mathcal{B}_{X_i})$ **and** patience $\leq \rho$ **do**

3: Let $X_m \in \mathbf{V} \setminus (\{X_i\} \cup \tilde{\mathcal{M}}\mathcal{B}_{X_i})$ be a variable minimizing $H(X_i | \tilde{\mathcal{M}}\mathcal{B}_{X_i} \cup \{X_m\})$. $\{ \triangleright H(\cdot | \cdot) \}$ is estimated via Eq. 6 or Eq. 1

4: **if** $H(X_i | \tilde{\mathcal{M}}\mathcal{B}_{X_i}) - H(X_i | \tilde{\mathcal{M}}\mathcal{B}_{X_i} \cup \{X_m\}) > \epsilon_g$ **then**

5: patience $\leftarrow 0$.

6: **else**

7: patience \leftarrow patience + 1.

8: **end if**

9: $\tilde{\mathcal{M}}\mathcal{B}_{X_i} \leftarrow \tilde{\mathcal{M}}\mathcal{B}_{X_i} \cup \{X_m\}$.

10: **end while**

Shrinking phase

11: **while** $\tilde{\mathcal{M}}\mathcal{B}_{X_i} \neq \emptyset$ **do**

12: Let $X_m \in \tilde{\mathcal{M}}\mathcal{B}_{X_i}$ be a variable minimizing $\delta_H = H(X_i | \tilde{\mathcal{M}}\mathcal{B}_{X_i} \setminus \{X_m\}) - H(X_i | \tilde{\mathcal{M}}\mathcal{B}_{X_i})$.

13: **if** $\delta_H > \epsilon_s$ **then**

14: **break**

15: **end if**

16: $\tilde{\mathcal{M}}\mathcal{B}_{X_i} \leftarrow \tilde{\mathcal{M}}\mathcal{B}_{X_i} \setminus \{X_m\}$.

17: **end while**

weights poorly reflect true dependencies, for which mutual information performs better, leading to optimization errors that propagate in later DAG search. Multiple configurations of $W_{i,j}^n$ can yield nearly identical values of $\mathcal{L}_n(\theta_n)$, reducing reliability. Building upon SDCD [26], we introduce **FANSITE-DCD**, which leverages **FANSITEMB**-inferred MBs to construct a moral graph used as a mask. Masking on this moral graph allows the DAG search in the later stage to continue removing redundant edges under DAG constraints (e.g., eliminating reverse edges and spouse links). The neural network and DAG penalty score from SDCD are utilized to support this process. While **FANSITE-DCD** improves upon DCD, it can also serve as a moral-graph-based initialization step for other causal discovery methods.

Definition 6 (Moral graph). The moral graph $\mathcal{M}[\mathcal{G}]$ of a Bayesian network \mathcal{G} with variables in \mathbf{V} and an underlying positive distribution P is the undirected graph over \mathbf{V} containing edges between each variable X_i and variables in its MB. $\mathcal{M}[\mathcal{G}]$ serves as the *unique minimal I-map* for P [18].

Remark 7. An I-map for P is any graph \mathcal{K} with its set of conditional independencies (CI) $\mathcal{I}(\mathcal{K})$ satisfying $\mathcal{I}(\mathcal{K}) \subseteq \mathcal{I}$, where \mathcal{I} is the CI set associated with P (i.e., $X \perp\!\!\!\perp Y | \mathbf{Z}$).

From Definition 3.13 in [18] and Definition 6, we deduce that the moral graph $\mathcal{M}[\mathcal{G}]$ is the *sparsest I-map*, with $\mathcal{I}(\mathcal{K}) \subseteq \mathcal{I}(\mathcal{M}[\mathcal{G}])$ for all \mathcal{K} . Thus, if the MBs of all variables are accurately recovered, the induced moral graph establishes a substantially reduced space for DAG search, forming a *minimal I-map-based subspace*.

Proposition 8. *Under the conditions stated in Theorem 5, FANSITE-DCD utilizes observational data to search for the optimal DAG within a minimal I-map-based subspace, rather than starting from the larger space of all I-maps. This approach enables it to converge more accurately and quickly to a DAG $\hat{\mathcal{G}}$ that is I-Markov-equivalent to the true DAG \mathcal{G}^* .*

This proposition is direct facilitated by our Theorem 5, following Definition 6 for moral graphs.

IV. EXPERIMENTS

A. Methods

For **MB discovery**, we evaluate: (1) constraint-based approaches, including IAMB [38], which dynamically selects the most associated features to the target conditioned on selected ones, and TC [32], which prunes edges by conditioning on all remaining variables; (2) score-based methods such as S²TMB [14], leveraging the coexistence of spouses and descendants alongside decomposable Bayesian scores, and kernel-based KMB [43], minimizing a conditional covariance operator; (3) Hybrid approaches like EEMB [42], combining CI tests for parent-child discovery with S²TMB scores for spouse discovery; and (4) DAT-Moral, which serves as the MB preselection stage using sparse regression in DAT [2].

For **causal discovery**, we assess three strategies: (1) MB-informed constraint-based methods like MARVEL [25], using recursive learning via removable variables; (2) plain differentiable causal discovery (DCD) such as DAGMA [3], which employs log-determinant acyclicity constraint, and COSMO [24], a constraint-free approach using an orientation matrix; and (3) MB-based DCD identifying MBs in the preselection stage using sparse regression, consisting of SDCD [26], which uses a neural autoencoder and minimizes negative log-likelihood in later DAG estimation, while DAT [2] trains an amortized model to learn separating sets and applies differentiable adjacency tests for edge pruning. We adopt default configurations recommended by respective baseline methods. For our approach, we utilize our class of masked autoregressive flows **FANS** as the conditional entropy estimator for nonlinear and real data, while using Eq. 1 for linear Gaussian cases.

B. Datasets

1) *Synthetic data*: The process for generating synthetic data strictly follows public code from the *gcastle* package.⁴ Erdős-Rényi causal DAGs are generated with node counts $d \in \{30, 100, 1000, 5000\}$ for both linear and nonlinear Gaussian SEMs, with weighted adjacency matrices constructed using edge weights randomly sampled from $\mathcal{U}([-2, -0.5] \cup [0.5, 2])$. Linear data is generated using the

linear SEM model $\mathbf{X} = \mathbf{W}^T \mathbf{X} + \epsilon$, where $\epsilon \sim \mathcal{N}(0, 1)$, while nonlinear data is generated following $X_i = f_i(X_{Pa_i}) + \epsilon_i$, where f_i is sampled from a Gaussian Process with an RBF kernel of bandwidth 1. For each setting, five datasets are sampled, each containing the ground truth adjacency matrix of the causal DAG, a training dataset of 1000 samples for $d < 100$, and 5000 samples for $d \geq 100$. All evaluation scenarios include (1) linear SEMs: sparse graphs {d30, d100-1, d1000} with average degree $\bar{D} = 1$, dense graphs d100-2 with $\bar{D} = 6$, and large graphs d5000 with $\bar{D} = 1.5$, and (2) nonlinear SEMs: {d30-G, d100-1} with $\epsilon_i \sim \mathcal{N}(0, 1)$, and d30-Mixed-noises (d30-MN) with $\epsilon_i \sim p_{\epsilon_i}$, where $p_{\epsilon_i} \in \{\mathcal{N}(0, 1), \mathcal{U}(-1, 1), \text{Laplace}(0, 1), \text{Gumbel}(0, 1), \text{Exp}(0, 1)\}$.

2) *Real and semi-real networks*: We use four public real-world/semi-real gene regulatory networks (GRN): (1) Sachs [34], a protein interaction network with expression data for proteins and phospholipids in human cells; (2) SynTReN [40], the semi-synthetic GRN based on real topologies and Michaelis-Menten/Hill kinetics; (3) SERGIO [10], the simulated gene expression dataset using high-throughput scRNA-seq technologies guided by real GRNs (we use 3,000 single cells, three bins each, and stochastic noise modeled via the Dual Production Decay framework); and (4) ARTH150 [28], an Arabidopsis thaliana GRN from the *bnlearn*⁵ repository.

TABLE I. Real datasets

Dataset	Nodes	Edges	Observations
Sachs [34]	11	17	853
SynTReN [40]	20	24	500
SERGIO [10]	100	137	9000
ARTH150 [28]	107	150	5000

C. Evaluation metrics

MB evaluation: In addition to F1 score, two ranking metrics from information retrieval are employed: (1) nDCG (Normalized Discounted Cumulative Gain), and (2) AveP (Average Precision). We observe that most surveyed MB discovery methods evolve their predicted MBs by approaching variables from most to least probable. To facilitate this, we do not alter the order of variables in the MB when running the compared algorithms. In principle, a higher nDCG/AveP is reported when variables in the true MB are positioned closer to the top of the predicted list. We report the average results of F1, nDCG, and AveP across all MBs of variables in the network.

Causal discovery thresholding & evaluation: For DCD methods, we follow standard CD practices by setting a final threshold on post-training score adjacency matrices to ensure DAG outputs [3], [24], [26]. We utilize three metrics that compare the estimated DAG with the ground truth: (1) AUCPR (area under the curve of precision-recall), (2) AUC-ROC (area under the receiver operating characteristic curve), and (3) SHD (Structural Hamming Distance), which refers to the minimum number of edge additions, deletions, and reversals required to transform the recovered DAG into the true DAG.

⁴<https://github.com/huawei-noah/trustworthyAI>

⁵<https://www.bnlearn.com/>

TABLE II. **Markov boundary discovery performance in %**. The numbers are *mean ± standard deviation* over 5 independent simulations, except for real data. Missing entries (–) correspond to instances with runtime exceeding the limit of 10 hours. **Bold**: best performance, *italic*: second-best performance.

Graph type	Metric	IAMB [38]	S2TMB [14]	EEMB [42]	TC [32]	KMB [43]	DAT-Moral [2]	FANSITEMB (ours)
Linear data								
d30	nDCG (↑)	47.18 ± 12.81	93.01 ± 3.74	90.78 ± 6.54	98.91 ± 1.25	70.58 ± 7.60	90.00 ± 3.84	99.34 ± 1.02
	AveP (↑)	40.34 ± 15.41	90.56 ± 5.11	87.42 ± 8.93	<u>98.42 ± 1.81</u>	60.69 ± 9.57	86.14 ± 5.17	99.08 ± 1.39
	F1 (↑)	48.25 ± 12.72	93.58 ± 3.79	91.39 ± 6.40	<u>98.68 ± 1.72</u>	65.36 ± 7.04	21.28 ± 3.22	99.44 ± 0.87
d100-1	nDCG (↑)	41.71 ± 5.36	94.27 ± 1.90	96.01 ± 2.00	99.90 ± 0.22	–	97.42 ± 1.34	99.86 ± 0.22
	AveP (↑)	34.54 ± 5.37	91.80 ± 2.74	94.29 ± 2.88	99.85 ± 0.34	–	96.33 ± 1.72	99.78 ± 0.33
	F1 (↑)	42.87 ± 5.64	95.60 ± 1.73	96.64 ± 1.91	<u>98.59 ± 0.60</u>	–	22.33 ± 1.14	99.88 ± 0.18
d100-2	nDCG (↑)	38.69 ± 3.11	42.69 ± 2.74	20.13 ± 1.05	<u>83.43 ± 9.49</u>	–	45.58 ± 6.08	97.12 ± 0.34
	AveP (↑)	19.81 ± 2.60	26.33 ± 1.83	8.07 ± 0.51	<u>75.17 ± 13.92</u>	–	25.82 ± 6.01	95.65 ± 0.54
	F1 (↑)	40.99 ± 2.12	46.39 ± 2.43	19.27 ± 0.88	<u>78.09 ± 10.98</u>	–	57.01 ± 2.78	97.38 ± 0.32
d1000	nDCG (↑)	43.53 ± 1.79	96.20 ± 0.59	96.45 ± 0.33	99.98 ± 0.02	–	99.10 ± 0.28	99.96 ± 0.05
	AveP (↑)	36.58 ± 1.95	94.90 ± 0.78	94.93 ± 0.47	99.97 ± 0.03	–	98.64 ± 0.42	99.93 ± 0.07
	F1 (↑)	45.50 ± 1.71	<u>96.82 ± 0.49</u>	96.76 ± 0.30	87.06 ± 1.40	–	45.05 ± 1.62	99.96 ± 0.04
d5000	nDCG (↑)	–	88.11 ± 1.08	87.8 ± 1.13	61.58 ± 0.72	–	–	99.59 ± 0.09
	AveP (↑)	–	<u>83.87 ± 1.43</u>	82.89 ± 1.52	50.73 ± 0.77	–	–	99.37 ± 0.14
	F1 (↑)	–	<u>89.75 ± 0.95</u>	88.65 ± 1.06	52.89 ± 0.76	–	–	99.61 ± 0.09
Nonlinear data								
d30-G	nDCG (↑)	29.25 ± 10.20	56.76 ± 9.78	56.57 ± 10.14	55.67 ± 10.22	68.50 ± 7.43	80.88 ± 4.59	93.5 ± 1.63
	AveP (↑)	22.81 ± 9.33	48.28 ± 10.30	48.05 ± 10.83	47.23 ± 11.29	59.00 ± 8.26	74.11 ± 5.77	90.58 ± 2.23
	F1 (↑)	30.49 ± 9.82	58.8 ± 9.20	59.06 ± 9.65	55.52 ± 10.05	<u>61.84 ± 8.26</u>	21.28 ± 3.22	91.2 ± 2.08
d30-MN	nDCG (↑)	27.33 ± 7.26	52.24 ± 2.75	54.44 ± 3.07	53.13 ± 4.32	61.66 ± 5.50	76.60 ± 7.45	90.67 ± 4.85
	AveP (↑)	20.98 ± 4.46	43.63 ± 3.80	45.94 ± 4.53	45.20 ± 5.39	51.69 ± 5.80	<u>69.01 ± 8.23</u>	86.56 ± 6.44
	F1 (↑)	28.19 ± 9.12	54.99 ± 2.58	<u>56.09 ± 2.95</u>	52.66 ± 3.93	55.32 ± 5.72	21.28 ± 3.22	87.72 ± 6.12
d100-1	nDCG (↑)	33.07 ± 4.80	65.21 ± 3.64	65.28 ± 3.42	70.83 ± 3.68	–	87.91 ± 5.20	90.91 ± 2.41
	AveP (↑)	26.41 ± 3.83	56.61 ± 3.42	56.71 ± 3.22	62.83 ± 4.01	–	<u>83.20 ± 6.97</u>	86.72 ± 3.51
	F1 (↑)	34.02 ± 5.64	67.90 ± 3.71	68.03 ± 3.28	67.10 ± 3.27	–	59.00 ± 1.04	87.54 ± 3.00
Real/Semi-real networks								
Sachs	nDCG (↑)	25.04	60.84	60.84	64.36	<u>73.22</u>	70.2	86.44
	AveP (↑)	17.2	49.42	49.42	53.96	64.2	60.08	80.44
	F1 (↑)	21.42	61.05	61.05	64.08	<u>64.68</u>	58.17	84.48
SynTReN	nDCG (↑)	16.13	31.72	29.3	22.79	22.27	33.96	68.36
	AveP (↑)	11.08	28.1	26.22	20.16	21.3	<u>31.59</u>	64.39
	F1 (↑)	9.52	31.35	31.48	31.31	21.67	<u>33.03</u>	68.18
SERGIO	nDCG (↑)	45.03	–	–	38.11	–	14.70	85.93
	AveP (↑)	<u>42.42</u>	–	–	35.01	–	12.63	82.56
	F1 (↑)	<u>33.75</u>	–	–	14.03	–	5.51	84.16
ARTH150	nDCG (↑)	35.56	93.58	<u>94.12</u>	92.55	–	79.73	96.66
	AveP (↑)	31.5	91.27	<u>92.19</u>	91.36	–	76.72	95.97
	F1 (↑)	36.32	<u>94.54</u>	94.52	90.49	–	38.48	96.12

TABLE III. **Causal discovery performance**. The numbers are *mean ± standard deviation* over 5 independent simulations, except for real data. **Bold**: best performance, *italic*: second-best performance.

Graph type	Metric	DAGMA [3]	COSMO [24]	SDCD [26]	DAT [2]	MARVEL [25]	FANSITE-DCD (ours)
Nonlinear data							
d30-G	SHD (↓)	15.4 ± 8.85	25 ± 5.66	13 ± 5.43	420.2 ± 7.50	24.6 ± 6.23	12.8 ± 6.53
	AUC-ROC (↑)	0.752 ± 0.095	0.822 ± 0.084	<u>0.858 ± 0.074</u>	0.502 ± 0.068	0.603 ± 0.039	0.902 ± 0.045
	AUC-PR (↑)	0.488 ± 0.172	0.375 ± 0.077	<u>0.570 ± 0.144</u>	0.036 ± 0.013	0.144 ± 0.061	0.592 ± 0.098
d30-MN	SHD (↓)	21.8 ± 7.82	48.4 ± 12.46	30.6 ± 9.81	419.8 ± 6.10	26.6 ± 8.91	18.2 ± 8.14
	AUC-ROC (↑)	0.654 ± 0.066	0.777 ± 0.058	0.766 ± 0.037	0.488 ± 0.061	0.578 ± 0.041	0.866 ± 0.044
	AUC-PR (↑)	0.252 ± 0.118	0.207 ± 0.071	<u>0.259 ± 0.065</u>	0.034 ± 0.011	0.113 ± 0.062	0.466 ± 0.121
d100-1	SHD (↓)	58.8 ± 7.46	39.4 ± 4.98	38 ± 6.24	80.6 ± 9.26	86.8 ± 10.31	25.6 ± 2.3
	AUC-ROC (↑)	0.712 ± 0.023	0.815 ± 0.035	<u>0.822 ± 0.044</u>	0.652 ± 0.027	0.604 ± 0.029	0.920 ± 0.021
	AUC-PR (↑)	0.386 ± 0.042	<u>0.592 ± 0.069</u>	0.590 ± 0.102	0.118 ± 0.033	0.113 ± 0.039	0.694 ± 0.054
Real/Semi-real networks							
Sachs	SHD (↓)	14	15	13	37	16	10
	AUC-ROC (↑)	0.57	0.58	0.63	0.65	0.52	0.73
	AUC-PR (↑)	0.2	0.22	<u>0.28</u>	0.2	0.16	0.45
SynTReN	SHD (↓)	28	36	37	32	29	19
	AUC-ROC (↑)	0.59	0.65	0.6	0.53	0.51	0.82
	AUC-PR (↑)	0.12	<u>0.14</u>	0.1	0.07	0.06	0.42

D. Main results

Effectiveness of proposed methods **FANSITEMB** and **FANSITE-DCD** across various settings is shown in Tables II and III. Performance is reported for scenarios within a 10-hour time limit (otherwise shown with a dash “—”). In both tasks, **FANSITEMB** and **FANSITE-DCD** consistently achieve best or second-best results. In the MB discovery task, **FANSITEMB** significantly outperforms other baselines by a large margin in challenging scenarios, including dense graphs (d100-1), super-large graphs (d5000), nonlinear settings, and real networks, due to two advantages: (1) a universal score estimator capturing complex relationships and varied noise distributions, and (2) a straightforward greedy strategy for evolving MBs in poly-time. S²TMB, EEMB and TC show competitive performance on linear data thanks to solid convergence foundations of constraint-based groups but struggle with nonlinear data because of restricted score criteria. Moral-DAT and KMB perform better in nonlinear settings and real networks but receive low F1 scores due to sensitive thresholds/stop conditions. In the CD task, focus primarily lies on nonlinear settings due to their greater challenge. SDCD serves as SOTA among previous methods, surpassed by **FANSITE-DCD**, which incorporates **FANSITEMB** to better warm-start the subsequent DAG recovery stage from a substantially reduced search space.

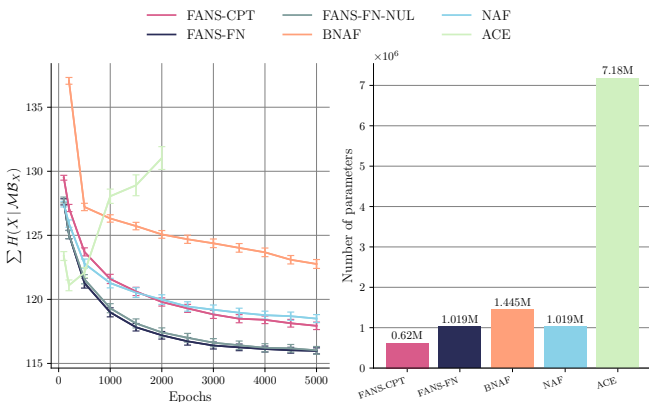


Fig. 2. Different model options for estimating our score criterion—conditional entropy. Experiments conducted on synthetic nonlinear graphs with $d = 100$. FANS-CPT, FANS-FN, and FANS-FN-NUL represent three variants in our proposed class of masked autoregressive flows (MAFs) tailored for MB discovery, corresponding to: a compact version with leaf masks, a non-compact version with leaf-masks, and a non-compact version without leaf masks. NAF and BNAF are typical MAF classes, while ACE [37] represents a class of energy-based estimators. The left figure illustrates the reduction across training epochs of $\sum H(X | \mathcal{MB}_X)$, which is the total conditional entropy as each variable conditions on its MB—smaller values indicate better performance. The right figure shows the number of trainable parameters; fewer parameters imply greater efficiency. When FANS is fully parameterized and trained with leaf-masking (FANS-FN), it learns even better than the compact counterpart. However, the compact FANS, with half the parameters of NAF, is expressive enough to surpass NAF in training and estimation, demonstrating the efficacy of our FANS class, as discussed in Subsection III-B2.

V. CONCLUSION

This paper presents an efficient score-based framework for Markov boundary (MB) discovery, employing conditional entropy from information-theoretic learning to facilitate score

objective design. A novel class of autoregressive flows is introduced to capture complex dependencies and noise distributions, accompanied by a theoretically guaranteed greedy parallelizable search in poly-time, ensuring robustness, scalability, and reliability in challenging high-dimensional and nonlinear settings. Experiments on synthetic and real bio-genetic datasets demonstrate the method’s superior performance in both MB and causal discovery tasks. As MB discovery is fundamental for tasks such as feature selection and causal inference, this advancement offers a versatile and promising solution for these critical data mining problems.

REFERENCES

- [1] C. F. Aliferis, A. Statnikov, I. Tsamardinos, S. Mani, and X. D. Koutsoukos. Local causal and Markov blanket induction for causal discovery and feature selection for classification part I: Algorithms and empirical evaluation. *JMLR*, 11:171–234, 2010.
- [2] Alan Nawzad Amin and Andrew Gordon Wilson. Scalable and flexible causal discovery with an efficient test for adjacency. In *Proc. of ICML*, pages 1331–1358, 2024.
- [3] Kevin Bello, Bryon Aragam, and Pradeep Ravikumar. DAGMA: Learning DAGs via M-matrices and a log-determinant acyclicity characterization. In *NeurIPS*, pages 8226–8239, 2022.
- [4] Asic Chen, Rui’an Ian Shi, Xiang Gao, Ricardo Baptista, and Rahul G Krishnan. Structured neural networks for density estimation and causal inference. In *NeurIPS*, pages 66438–66450, 2023.
- [5] Lin Chen, Moran Feldman, and Amin Karbasi. Weakly submodular maximization beyond cardinality constraints: Does randomization help greedy? In *Proc. of ICML*, pages 804–813, 2018.
- [6] Yuxin Chen, S Hamed Hassani, Amin Karbasi, and Andreas Krause. Sequential information maximization: When is greedy near-optimal? In *Proc. of COLT*, pages 338–363, 2015.
- [7] T. M. Cover. *Elements of information theory*. John Wiley & Sons, 1999.
- [8] Abhimanyu Das and David Kempe. Submodular meets spectral: Greedy algorithms for subset selection, sparse approximation and dictionary selection. In *Proc. of ICML*, pages 1057–1064, 2011.
- [9] Nicola De Cao, Wilker Aziz, and Ivan Titov. Block neural autoregressive flow. In *Proc. of UAI*, pages 1263–1273, 2020.
- [10] P. Dibaeinia and S. Sinha. SERGIO: A single-cell expression simulator guided by gene regulatory networks. *Cell systems*, 11:252–271, 2020.
- [11] Shuyu Dong, Michele Sebag, Kento Uemura, Akito Fujii, Shuang Chang, Yusuke Koyanagi, and Koji Maruhashi. DCILP: A distributed approach for large-scale causal structure learning. In *Proc. of AAAI*, pages 16345–16353, 2025.
- [12] Bao Duong and Thin Nguyen. Diffeomorphic information neural estimation. In *Proc. of AAAI*, pages 7468–7475, 2023.
- [13] Jonathan Frankle and Michael Carbin. The lottery ticket hypothesis: Finding sparse, trainable neural networks. In *Proc. of ICLR*, 2019.
- [14] Tian Gao and Qiang Ji. Efficient score-based Markov blanket discovery. *International Journal of Approximate Reasoning*, 80:277–293, 2017.
- [15] Mathieu Germain, Karol Gregor, Iain Murray, and Hugo Larochelle. MADE: Masked autoencoder for distribution estimation. In *Proc. of ICML*, pages 881–889, 2015.
- [16] Inês Hipólito, Maxwell JD Ramstead, Laura Convertino, Anjali Bhat, Karl Friston, and Thomas Parr. Markov blankets in the brain. *Neuroscience & Biobehavioral Reviews*, 125:88–97, 2021.
- [17] Chin-Wei Huang, David Krueger, Alexandre Lacoste, and Aaron Courville. Neural autoregressive flows. In *Proc. of ICML*, pages 2078–2087, 2018.
- [18] Daphne Koller and Nir Friedman. *Probabilistic graphical models: Principles and techniques*. MIT press, 2009.
- [19] Yang Li. *Moral Markov blankets: An investigation of some properties and value for machine learning*. PhD thesis, Monash University, 2020.
- [20] Chenxi Liu, Yongqiang Chen, Tongliang Liu, Mingming Gong, James Cheng, Bo Han, and Kun Zhang. Discovery of the hidden world with large language models. In *NeurIPS*, 2024.
- [21] Wei Liu, Yi Jiang, Li Peng, Xingen Sun, Wenqing Gan, Qi Zhao, and Huanrong Tang. Inferring gene regulatory networks using the improved Markov blanket discovery algorithm. *Interdisciplinary Sciences: Computational Life Sciences*, 14:168–181, 2022.

- [22] Yang Liu and Anthony Constantinou. Improving the imputation of missing data with Markov blanket discovery. In *Proc. of ICLR*, 2022.
- [23] Dimitris Margaritis and Sebastian Thrun. Bayesian network induction via local neighborhoods. In *NeurIPS*, 1999.
- [24] Riccardo Massidda, Francesco Landolfi, Martina Cinquini, and Davide Bacciu. Constraint-free structure learning with smooth acyclic orientations. In *Proc. of ICLR*, 2024.
- [25] Ehsan Mokhtarian, Sepehr Elahi, Sina Akbari, and Negar Kiyavash. Recursive causal discovery. *JMLR*, 26:1–65, 2025.
- [26] A. Nazaret, J. Hong, E. Azizi, and D. Blei. Stable differentiable causal discovery. In *Proc. of ICML*, pages 37413–37445, 2024.
- [27] Teppo Niinimäki and Pekka Parviainen. Local structure discovery in Bayesian networks. In *Proc. of UAI*, pages 634–643, 2012.
- [28] R. Opgen-Rhein and K. Strimmer. From correlation to causation networks: A simple approximate learning algorithm and its application to high-dimensional plant gene expression data. *BMC systems biology*, 1:1–10, 2007.
- [29] George Papamakarios, Eric Nalisnick, Danilo Jimenez Rezende, Shakir Mohamed, and Balaji Lakshminarayanan. Normalizing flows for probabilistic modeling and inference. *JMLR*, 22:1–64, 2021.
- [30] George Papamakarios, Theo Pavlakou, and Iain Murray. Masked autoregressive flow for density estimation. In *NeurIPS*, 2017.
- [31] Judea Pearl. *Causality: Models, Reasoning and Inference*. Cambridge University Press, 2009.
- [32] Jean-Philippe Pellet and André Elisseeff. Using Markov blankets for causal structure learning. *JMLR*, 9:1295–1342, 2008.
- [33] M. Raffa. Markov blankets for sustainability. In *Proc. of SEFM*, pages 313–323, 2022.
- [34] Karen Sachs, Omar Perez, Dana Pe’er, Douglas A Lauffenburger, and Garry P Nolan. Causal protein-signaling networks derived from multiparameter single-cell data. *Science*, 308:523–529, 2005.
- [35] Dravyansh Sharma, Ashish Kapoor, and Amit Deshpande. On greedy maximization of entropy. In *Proc. of ICML*, pages 1330–1338, 2015.
- [36] Andy Shih, Dorsa Sadigh, and Stefano Ermon. Training and inference on any-order autoregressive models the right way. In *NeurIPS*, pages 2762–2775, 2022.
- [37] Ryan Strauss and Junier B Oliva. Arbitrary conditional distributions with energy. In *NeurIPS*, pages 752–763, 2021.
- [38] I. Tsamardinos and C. F. Aliferis. Towards principled feature selection: Relevancy, filters and wrappers. In *AISTATS*, pages 300–307, 2003.
- [39] Ioannis Tsamardinos, Constantin F Aliferis, Alexander R Statnikov, and Er Statnikov. Algorithms for large scale Markov blanket discovery. In *Proc. of FLAIRS*, pages 376–81, 2003.
- [40] T. Van den Bulcke, K. Van Leemput, B. Naudts, P. van Remortel, H. Ma, A. Verschoren, B. De Moor, and K. Marchal. SynTREN: A generator of synthetic gene expression data for design and analysis of structure learning algorithms. *BMC bioinformatics*, 7:1–12, 2006.
- [41] Matthew J Vowels, Necati Cihan Camgoz, and Richard Bowden. Dya like DAGs? A survey on structure learning and causal discovery. *ACM Computing Surveys*, 55:1–36, 2022.
- [42] Hao Wang, Zhaolong Ling, Kui Yu, and Xindong Wu. Towards efficient and effective discovery of Markov blankets for feature selection. *Information Sciences*, 509:227–242, 2020.
- [43] Xingyu Wu, Bingbing Jiang, Tianhao Wu, and Huanhuan Chen. Practical Markov boundary learning without strong assumptions. In *Proc. of AAAI*, pages 10388–10398, 2023.
- [44] Kui Yu, Lin Liu, and Jiuyong Li. A unified view of causal and non-causal feature selection. *TKDD*, 15:1–46, 2021.

APPENDIX A
PROOFS FROM THE SECTION III

A. *Proof of theorem 2*

Theorem 2. Let $T \in \mathbf{V}$ be a random variable and let $\mathcal{MB}_T \subset \mathbf{V}$ denote its Markov boundary. Under causal sufficiency and the faithfulness condition, the Markov boundary \mathcal{MB}_T of the target variable T is the unique minimal subset $\mathbf{S} \subseteq \mathbf{V} \setminus \{T\}$ that minimizes the conditional entropy $H(T | \mathbf{S})$. Furthermore, for any subset $\mathbf{S}' \subseteq \mathbf{V} \setminus \{T\}$ such that $\mathcal{MB}_T \subseteq \mathbf{S}'$, it holds that $H(T | \mathbf{S}') = H(T | \mathcal{MB}_T)$.

Proof.

By Theorem 2 in [44], under causal sufficiency and the faithfulness condition, the Markov boundary \mathcal{MB}_T of T is the unique minimal subset of $\mathbf{V} \setminus \{T\}$ that maximizes the mutual information $I(T; \mathbf{S})$ over all subsets $\mathbf{S} \subseteq \mathbf{V} \setminus \{T\}$.

By the definition of mutual information,

$$I(T; \mathbf{S}) = H(T) - H(T | \mathbf{S}), \quad (8)$$

where $H(T)$ is the entropy of T and $H(T | \mathbf{S})$ is the conditional entropy of T given \mathbf{S} . Since $H(T)$ is independent of the choice of \mathbf{S} , maximizing $I(T; \mathbf{S})$ is equivalent to minimizing $H(T | \mathbf{S})$. Therefore,

$$\mathcal{MB}_T = \arg \min_{\mathbf{S} \subseteq \mathbf{V} \setminus \{T\}} H(T | \mathbf{S}), \quad (9)$$

and \mathcal{MB}_T is the unique minimal subset with this property.

Now, consider any subset $\mathbf{S}' \subseteq \mathbf{V} \setminus \{T\}$ such that $\mathcal{MB}_T \subseteq \mathbf{S}'$. By the property that conditioning on a larger set cannot increase conditional entropy, we have

$$H(T | \mathbf{S}') \leq H(T | \mathcal{MB}_T). \quad (10)$$

Since \mathcal{MB}_T is a minimizer, equality must hold:

$$H(T | \mathbf{S}') = H(T | \mathcal{MB}_T). \quad (11)$$

■

B. *Proof of theorem 4*

Theorem 4. Assume the existence of a universal conditional entropy approximator \mathcal{F}_θ^* . Let the forward phase of Algorithm 1 yield $\tilde{\mathcal{MB}}_{X_i}^+$, with $|\tilde{\mathcal{MB}}_{X_i}^+| = k'$. Denote the true Markov boundary of X_i as \mathcal{MB}_{X_i} with $|\mathcal{MB}_{X_i}| = k$. For any $\delta_e > 0$,

$$0 \leq H(X_i | \tilde{\mathcal{MB}}_{X_i}^+) - H(X_i | \mathcal{MB}_{X_i}) \leq \delta_e + \Delta_N \quad (12)$$

where

$$\Delta_N := \log N \left[1 - \exp \left(- \frac{k'}{k\gamma \max\{\log N, \log(1/\delta_e)\}} \right) \right],$$

and γ reflects measurement noise for N samples.

For the linear Gaussian case, where the conditional entropy $H(T | \mathbf{S})$ has the closed form

$$H(T | \mathbf{S}) = \frac{1}{2} \left(1 + \log(2\pi) + \log \frac{\det \boldsymbol{\Sigma}_{\{T\} \cup \mathbf{S}}}{\det \boldsymbol{\Sigma}_{\mathbf{S}}} \right), \quad (13)$$

define:

$$\begin{aligned} A &:= 2\pi e \sigma_{X_i}^2 - \exp(2H(X_i | \mathcal{MB}_{X_i})) \\ A' &:= 2\pi e \sigma_{X_i}^2 - \exp(2H(X_i | \tilde{\mathcal{MB}}_{X_i}^+)) \end{aligned}$$

Then:

$$1 \leq \frac{A}{A'} \leq \frac{1}{1 - \exp(-\lambda_{\min}(\mathbf{C}, 2k'))} \quad (14)$$

where σ_{X_i} is the standard deviation of X_i , and $\lambda_{\min}(\mathbf{C}, 2k')$ is the minimum eigenvalue among all $2k' \times 2k'$ sub-matrices of the joint correlation matrix \mathbf{C} .

Proof.

We first consider the general case. Assume the density $p(x)$ of any X is Riemann integrable. By the limiting density of discrete points (LDDP) theorem (Theorem 8.3.1, [7]), for sufficiently small bin width Δ ,

$$H_{\mathbb{S}}(X^\Delta) + \log \Delta \rightarrow H(X) \quad \text{as } \Delta \rightarrow 0, \quad (15)$$

where $H_{\mathbb{S}}(X^\Delta)$ is the Shannon entropy of the discretized variable. Therefore, the conditional entropy for continuous variable T and conditioning set \mathbf{S} can be approximated as

$$H(T | \mathbf{S}) = H(T, \mathbf{S}) - H(\mathbf{S}) \approx H_{\mathbb{S}}(T, \mathbf{S}) - H_{\mathbb{S}}(\mathbf{S}) = H_{\mathbb{S}}(T | \mathbf{S}). \quad (16)$$

This facilitates Theorem 2 in [6]. Specifically, for any $\delta_e > 0$, the Shannon mutual information satisfies:

$$I_{\mathbb{S}}(X_i; \tilde{\mathcal{M}}\mathcal{B}_{X_i}^+) \geq I_{\mathbb{S}}(X_i; \mathcal{M}\mathcal{B}_{X_i}) - \delta_e - \Delta_N, \quad (17)$$

where

$$\Delta_N := \log N \left[1 - \exp \left(-\frac{k'}{k\gamma \max\{\log N, \log(1/\delta_e)\}} \right) \right].$$

From Eq. 16 and Inequality 17, we can derive the upper bound in the general case:

$$0 \leq H(X_i | \tilde{\mathcal{M}}\mathcal{B}_{X_i}^+) - H(X_i | \mathcal{M}\mathcal{B}_{X_i}) \leq \delta_e + \Delta_N. \quad (18)$$

If we choose $k' \geq k\gamma \max\{\log N, \log(1/\delta_e)\} \ln \left(\frac{\log N}{\delta_e} \right)$ (i.e., sufficiently many queries in the forward pass of Algorithm 1), it follows directly from the analysis of Theorem 2 in [6] that

$$I_{\mathbb{S}}(X_i; \tilde{\mathcal{M}}\mathcal{B}_{X_i}^+) \geq I_{\mathbb{S}}(X_i; \mathcal{M}\mathcal{B}_{X_i}) - 2\delta_e,$$

which implies that: $H(X_i | \tilde{\mathcal{M}}\mathcal{B}_{X_i}^+) - H(X_i | \mathcal{M}\mathcal{B}_{X_i}) \leq 2\delta_e$.

Linear Gaussian Case.

Suppose $\mathbf{x}_{\mathbb{S}}$ are standardized to $\tilde{\mathbf{x}}_{\mathbb{S}}$. First, we prove that the entropy of a standardized Gaussian variable set \mathbf{S} is given by

$$\tilde{H}(\mathbf{S}) = H(\mathbf{S}) - \sum_j \log \sigma_j, \quad (19)$$

where σ_j is the standard deviation of $X_j \in \mathbf{S}$.

Denote $s := |\mathbf{S}|$. Let $\mathbf{x}_{\mathbf{S}} \sim \mathcal{N}(\boldsymbol{\mu}_{\mathbf{S}}, \boldsymbol{\Sigma}_{\mathbf{S}})$, where $\boldsymbol{\mu}_{\mathbf{S}} \in \mathbb{R}^s$ is the mean vector and $\boldsymbol{\Sigma}_{\mathbf{S}} \in \mathbb{R}^{s \times s}$ is the covariance matrix. The Gaussian entropy $H(\mathbf{S})$ is given by:

$$H(\mathbf{S}) = \frac{1}{2} \log ((2\pi e)^s \det(\boldsymbol{\Sigma}_{\mathbf{S}})). \quad (20)$$

Let $\mathbf{S} := \{X_{i_1}, X_{i_2}, \dots, X_{i_s}\}$ and let σ_j denote the standard deviation of X_j for all $j \in \{i_1, i_2, \dots, i_s\}$. Using the factorization $\boldsymbol{\Sigma}_{\mathbf{S}} = \mathbf{D}_{\mathbf{S}} \mathbf{C}_{\mathbf{S}} \mathbf{D}_{\mathbf{S}}$, where $\mathbf{D}_{\mathbf{S}} = \text{diag}(\sigma_{i_1}, \dots, \sigma_{i_s})$, and $\mathbf{C}_{\mathbf{S}}$ is sub-correlation matrix of \mathbf{C} corresponding to variables in \mathbf{S} from $\{X_1, X_2, \dots, X_d\}$, we get:

$$\det(\boldsymbol{\Sigma}_{\mathbf{S}}) = \det(\mathbf{D}_{\mathbf{S}})^2 \det(\mathbf{C}_{\mathbf{S}}) = \left(\prod_{j=1}^s \sigma_{i_j} \right)^2 \det(\mathbf{C}_{\mathbf{S}}). \quad (21)$$

So the entropy becomes:

$$H(\mathbf{S}) = \frac{1}{2} \log \left((2\pi e)^s \left(\prod_{j=1}^s \sigma_{i_j} \right)^2 \det(\mathbf{C}_{\mathbf{S}}) \right). \quad (22)$$

Now define the standardization:

$$\tilde{\mathbf{x}}_{\mathbf{S}} = \mathbf{D}_{\mathbf{S}}^{-1}(\mathbf{x}_{\mathbf{S}} - \boldsymbol{\mu}_{\mathbf{S}}) \sim \mathcal{N}(\mathbf{0}, \mathbf{C}_{\mathbf{S}}). \quad (23)$$

The entropy $\tilde{H}(\mathbf{S})$ corresponding to $\tilde{\mathbf{x}}_{\mathbf{S}}$ is:

$$\tilde{H}(\mathbf{S}) = \frac{1}{2} \log ((2\pi e)^s \det(\mathbf{C}_{\mathbf{S}})). \quad (24)$$

Now subtract:

$$\begin{aligned} H(\mathbf{S}) - \tilde{H}(\mathbf{S}) &= \frac{1}{2} \log \left((2\pi e)^s \left(\prod_{j=1}^s \sigma_{i_j} \right)^2 \det(\mathbf{C}_{\mathbf{S}}) \right) - \frac{1}{2} \log ((2\pi e)^s \det(\mathbf{C}_{\mathbf{S}})) \\ &= \frac{1}{2} \log \left(\left(\prod_{j=1}^s \sigma_{i_j} \right)^2 \right) = \log \left(\prod_{j=1}^s \sigma_{i_j} \right) = \sum_{j=1}^s \log \sigma_{i_j}. \end{aligned} \quad (25)$$

Next, let \mathbf{C}_S and $\mathbf{C}_{\{T\} \cup S}$ denote the sub-matrices of the correlation matrix \mathbf{C} corresponding to the variable sets S and $\{T\} \cup S$, respectively (i.e., the covariance matrix after standardization). From Lemma 3.6 in [8], we have:

$$\mathbf{C}_{\{T\} \cup S} = \begin{pmatrix} 1 & \mathbf{b}^\top \\ \mathbf{b} & \mathbf{C}_S \end{pmatrix}, \quad (26)$$

where \mathbf{b} is the covariance vector between T and variables in S .

The conditional entropy is then

$$\begin{aligned} H(T | S) &= H(T, S) - H(S) \\ &= \tilde{H}(T, S) + \log \sigma_T + \sum_{j=1}^s \log \sigma_{i_j} - \tilde{H}(S) - \sum_{j=1}^s \log \sigma_{i_j} \\ &= \tilde{H}(T, S) + \log \sigma_T - \tilde{H}(S) \\ &= \tilde{H}(T | S) + \log \sigma_T \\ &= \frac{1}{2} \left(1 + \log(2\pi) + \log \frac{\det \mathbf{C}_{\{T\} \cup S}}{\det \mathbf{C}_S} \right) + \log \sigma_T \\ &= \frac{1}{2} (1 + \log(2\pi) + \log(1 - \mathbf{b}^\top \mathbf{C}_S^{-1} \mathbf{b})) + \log \sigma_T \end{aligned} \quad (27)$$

It is easy to see that the forward pass procedure in our Algorithm 1 aligns with the forward regression (forward selection) process defined in Definition 3.1 of [8]. From Eq. 27, it can be deduced that minimizing our conditional entropy score $H(X_i | \tilde{\mathcal{M}}\mathcal{B}_{X_i}^+)$ is equivalent to maximizing the term

$$R_{X_i, \tilde{\mathcal{M}}\mathcal{B}_{X_i}^+}^2 := \mathbf{b}^\top \left(\mathbf{C}_{\tilde{\mathcal{M}}\mathcal{B}_{X_i}^+} \right)^{-1} \mathbf{b},$$

where \mathbf{b} is the covariance vector between X_i and variables in $\tilde{\mathcal{M}}\mathcal{B}_{X_i}^+$. Hence, from Theorem 3.2 in [8], it is straightforward to obtain:

$$R_{X_i, \tilde{\mathcal{M}}\mathcal{B}_{X_i}^+}^2 \geq (1 - \exp(-\lambda_{\min}(\mathbf{C}, 2k'))) R_{X_i, \mathcal{M}\mathcal{B}_{X_i}}^2, \quad (28)$$

where $R_{X_i, \mathcal{M}\mathcal{B}_{X_i}}^2$ corresponds to the optimal case. $R_{T, S}^2$ is weakly sub-modular [8].

Let:

$$A := 2\pi e \sigma_{X_i}^2 - \exp(2H(X_i | \mathcal{M}\mathcal{B}_{X_i})), \quad A' := 2\pi e \sigma_{X_i}^2 - \exp(2H(X_i | \tilde{\mathcal{M}}\mathcal{B}_{X_i}^+)).$$

From Eq. 27 and Inequality 28, it follows that

$$\frac{A}{A'} = \frac{R_{X_i, \mathcal{M}\mathcal{B}_{X_i}}^2}{R_{X_i, \tilde{\mathcal{M}}\mathcal{B}_{X_i}^+}^2} \leq \frac{1}{1 - \exp(-\lambda_{\min}(\mathbf{C}, 2k'))}, \quad (29)$$

where \mathbf{C} is the joint correlation matrix, i.e., the joint covariance matrix Σ of all variables after standardization.

The lower bound of 1 in Inequality 14 follows since $\mathcal{M}\mathcal{B}_{X_i}$ is the true minimizer of $H(X_i | S)$. ■

C. Proof of theorem 5

Theorem 5. Assume infinite observational data, faithfulness, causal sufficiency, and that \mathcal{F}_θ^* is a universal conditional entropy approximator. Then Algorithm 1 identifies exactly all variables in the Markov boundary of a target node.

Proof.

By our Theorem 4, under the stated conditions, the growing phase of Algorithm 1 guarantees that $\tilde{\mathcal{M}}\mathcal{B}_{X_i}^+$ contains the true Markov boundary if allowed to grow sufficiently large, i.e., $\mathcal{M}\mathcal{B}_{X_i} \subseteq \tilde{\mathcal{M}}\mathcal{B}_{X_i}^+$. Notably, for sparse Bayesian networks, the selection process may terminate early, yielding a relatively small $\tilde{\mathcal{M}}\mathcal{B}_{X_i}^+$ compared to the total number of variables.

We next demonstrate that the shrinking phase eliminates all extraneous variables, i.e., each $X_j \in \tilde{\mathcal{M}}\mathcal{B}_{X_i}^+ \setminus \mathcal{M}\mathcal{B}_{X_i}$, via induction on their count. At each iteration, a variable not in $\mathcal{M}\mathcal{B}_{X_i}$ is removed from $\tilde{\mathcal{M}}\mathcal{B}_{X_i}^+$, and this process continues until convergence. This follows directly, as removing any non-Markov boundary variable does not increase $H(X_i | \tilde{\mathcal{M}}\mathcal{B}_{X_i}^+)$, which already attains the minimum conditional entropy achievable (according to our Theorem 2). ■

APPENDIX B
REPRODUCTION DETAILS

Hyperparameter choice. We perform a grid-search to adopt best configurations. *Hyperparameters of FANS:* Transformer is a deep sigmoidal flow [17], with 1 layer and w, a, b as 4-dimensional vectors. Models are trained for up to 5000 epochs. Batch size is 64 for graphs with $d < 100$ and 256 for $d \geq 100$. In conditioner, output layer has 20 blocks for $d < 100$ and 16 for $d \geq 100$. One hidden layer with $\alpha_B = 6$ blocks is used for all d . For $d \geq 100$, compact version of **FANS** with $2 * M$ nodes per hidden block is used; non-compact version is used for $d < 100$. Maximum size of observed subsets: $M = d - 1$ for $d \leq 20$, $M = 20$ for $30 \leq d < 100$, and $M = 30$ for $d \geq 100$. *Hyperparameters of Algorithm 1:* $K = 1000$, $\epsilon_g = 0.005$, $\epsilon_s = 0.002$ for sparse graphs (node degree is less than 2); $\epsilon_g = \epsilon_s = 0.001$ for dense graphs, $\rho = 50$ for $d = 5000$ and $\rho = 15$ otherwise. Hyperparameters for DAG estimation in **FANSITE-DCD** set to defaults of SDCD [26]. Real/semi-real datasets are standardized beforehand.

Technical details. All experiments were conducted on Apple M3 CPU and A100 GPU.